Two fragments of HBV DNA integrated into chrX: 11009033 and its genetic regulation in HepG2.2.15

PENG RUAN[1], RUI ZHOU[1], CHUNPING HE[1], CHAO HUANG[1], MENGJUAN LIN[1], HAISEN YIN[1], XIUFANG DAI[2] and JUN SUN[1]

[1]Department of Gastroenterology, Renmin Hospital of Wuhan University, Wuhan, Hubei 430060; [2]Department of Breast Surgery, Renmin Hospital of Shiyan, Hubei University of Medicine, Shiyan, Hubei 442000, P.R. China

Received August 3, 2022; Accepted February 17, 2023

DOI: 10.3892/mmr.2023.12985

Abstract. Hepatitis B virus (HBV) integration into human genome causes hepatocellular carcinoma (HCC). The present study used inverse nested PCR; the full sequence of HBV DNA fragments of the chrX: 111009033 integration site was detected (987 bp), containing two fragments of double-stranded linear DNA with the same orientation (1,744-1,094 and 1,565-1,228 nt). By reverse transcription-quantitative PCR, HBV-cell fusion transcript was observed in HepG2.2.15 cells. The mean copy number of this site in cells with H_2O_2 treatment ($8.73x10^{-2}$±$1.65x10^{-2}$ copies/cell) was significantly higher than that in the cells without H_2O_2 treatment ($3.02x10^{-2}$±$2.33x10^{-2}$ copies/cell; P<0.0001). The mean levels of P21-activated kinase 3 (PAK3) were 15.67±5.65 copies/cell in HepG2.2.15 cells with H_2O_2 treatment, significantly higher than in the cells without H_2O_2 treatment (11.34±4.58 copies/cell, P=0.0076) and in HepG2 cells (5.92±1.54 copies/cell, P<0.0001). Significant difference of PAK3 levels was also found between HepG2.2.15 cells without H_2O_2 treatment and HepG2 cells (11.34±4.58 vs. 5.92±1.54 copies/cell, P<0.0001). The average copy numbers of the integration site chrX: 111009033 were positively correlated with the average levels of PAK3 (P=0.0013). The overall trend of PAK3 expression was significantly increased in HepG2.2.15 cells with H_2O_2 treatment compared with that in HepG2.2.15 cells without H_2O_2 treatment (37.63±8.16 and 31.38±7.94, P=0.008) and HepG2 cells (21.67±7.88, P<0.0001). In summary, the chrX: 11009033 integration site may originate from primary human hepatocytes, occurrence and clonal expansion of which may upregulate PAK3 expression, which may contribute to hepatocarcinogenesis.

Correspondence to: Dr Peng Ruan or Professor Jun Sun, Department of Gastroenterology, Renmin Hospital of Wuhan University, 238 Jiefang Road, Wuhan, Hubei 430060, P.R. China
E-mail: ruanpeng-1973@163.com
E-mail: 21709179@qq.com

Key words: hepatitis B virus integration, P21-activated kinase gene, hepatocellular carcinoma

Introduction

Hepatitis B virus (HBV) infection is a serious global public health problem especially in Africa and Asia, and is the cause of nearly 1 million deaths from liver disease each year (1). HBV is a small, enveloped, dsDNA virus with a full length of 3,200 bp. HBV covalently closed circular DNA (cccDNA) acts as the key intracellular replication template of the virus. Following infection of hepatocytes, HBV relaxed cDNA (rcDNA) enters the nucleus to form cccDNA pool using host proteins. During this period, HBV ds linear DNA (dslDNA) can integrate into the host genome when DNA strand breaks (DSBs) occur (2). HBV integration is one of the major pathogenic causes of HBV-associated hepatocellular carcinoma (HCC) and the second leading cause of cancer-associated death worldwide (3). The mechanisms may include chromosomal instability, dysfunction of cell cycle progression, host genes and apoptosis and increasing cell proliferation (4). However, due to the lack of *in vitro* infection models with detectable integration events, the molecular mechanism of the formation of HBV integration and its carcinogenic effects are not well-understood (5).

Traditional methods, such as Southern blotting and Alu-PCR, which are either time-consuming or laborious, have demonstrated that HBV DNA can randomly integrate into the host genome (6). Next generation sequencing (NGS) assay of HBV integration detection identified a large group of hotspots among the inserted host genes, for example, myeloid/lymphoid or mixed-lineage leukemia 4, telomerase reverse tranase (TERT), cyclin E1 (CCNE1) and lysine-specific methyltransferase 2B (KMT2B) (7-9). To the best of our knowledge, however, there remains a paucity of *in vitro* studies of these integration sites. P21-activated kinase 3 (PAK3) is an important oncogene in HCC (10); our previous study reported the HBV integration site chrX: 111009033, which inserted into PAK3 gene in HepG2.2.15 cells (11). The present study aimed to detect the full sequence of HBV DNA fragments of this site using an improved inverse nested PCR (invPCR), its genetic regulation and the expression of PAK3 protein in HepG2 and HepG2.2.15 cells with and without H_2O_2 treatment, which exacerbates HBV integration (12). The present study may help to elucidate the pathogenesis and carcinogenesis of chrX: 111009033 integration site.

Materials and methods

Cell culture. HepG2.2.15 and HepG2 liver cancer cells were purchased from China Center for Type Culture Collection (Wuhan, China). Cell lines were authenticated by STR identification and cultured with DMEM with 10% FBS (Sangon Biotech Co., Ltd.) and 200 μg/ml G418 (Sangon Biotech Co., Ltd.) at 37˚C with 5% CO_2. Subclones (termed C1-4) were transferred from parental cells to 4-well plates and expanded in culture to $5.0x10^6$-$1.0x10^7$ cells before collecting. Nuclear RNA and DNA from cells were extracted using the Genomic RNA and DNA Mini kits according to the manufacturer's instructions, respectively (both Sangon Biotech Co., Ltd.). For quantitative analysis of HBV integration and PAK3 gene, HepG2 and HepG2.2.15 cells (control group) were collected in 24-well plates at a density of $3.5x10^3$ cells/well. Additionally, as the treatment group, 24-well culture plates with HepG2.2.15 cells and H_2O_2 at 20 μmol/l were cultured, as previously described (12).

PCR and sequencing validation. The chrX: 111009033 integration site was detected by conventional PCR in HepG2.2.15 cells, with the primers forward (F)1 (5'-AGAGCCCCTGAG GGTTTT-3') and reverse (R)1 (5'-CCCGTCTGTGCCTTC TCA-3'). PCR mix was prepared with 10 μM F and R primers (1 μl each), 20 ng DNA (1 μl), 22 μl H_2O and 25 μl 2X Taq Buffer (Sangon Biotech Co., Ltd.), and thermocycling conditions were conducted as follows: Initial denaturation for 5 min at 95˚C followed by 40 cycles of denaturation for 10 sec at 95˚C, annealing for 10 sec at 54˚C and extension for 3 min at 72˚C and final extension for 10 min at 72˚C (11). The PCR products were electrophoresed (10 μg/lane) using a 1.3% agarose gel, extracted and sequenced by Sanger sequencing (Sangon Biotech Co., Ltd.). Finally, HBV-cell DNA junction was confirmed using Basic Local Alignment Search Tool (BLAST; https://blast.ncbi.nlm.nih.gov/Blast.cgi#alnHdr).

InvPCR. For verification of the full inserted HBV fragment of the chrX: 111009033 integration site, an improved invPCR (Fig. 1) was designed as described previously (13). Firstly, to amplify a chimeric fragment which partially aligned to host gene including Alu repeats and unknown integrated HBV gene, primer chimeric R (5'-AGCTTTTAATACCCAACTCCT CCC-3'), which included integrated HBV (1,732-1,744 nt) and PAK3 sequence (chrX111009033-111009027) and an Alu site (AGCT) at its 5' end, was designed. Because the orientation of the nearest Alu sequence is unknown, primers Alu F1 (5'-CGG ATCACCTGAGGTCAG-3') and Alu R1 (5'-ACGGAGTCT CGCTCTGTC-3') with opposite orientations were designed and added to two reaction mixes with primer chimeric R. The primer mix was prepared as aforementioned. Thermocycling conditions were as follows: Initial denaturation for 5 min at 95˚C followed by 40 cycles of denaturation for 10 sec at 95˚C, annealing for 10 sec at 56˚C and extension for 3 min at 72˚C and final extension for 10 min at 72˚C.

Secondly, the specific amplification product (1 μg) was digested with 1 μl Alu restriction enzyme [(New England BioLabs, Inc. (NEB)] for 1 h at 37˚C then inactivated for 20 min at 80˚C, followed by addition of 500 U T4 DNA ligase (NEB). The mixture was incubated at room temperature for 2 h, after which ligase was inactivated for 20 min at 80˚C, followed by purification using PCR Purification kit according to the manufacturer's protocol (Sangon Biotech Co., Ltd.). The DNA was divided into two parts for either double digestion with 5 U *Bsi*HKAI (1 h, 65˚C) and 5 U *Sph*I (1 h, 37˚C) or single digestion with 5 U *Bsi*HKAI (both NEB).

The digested DNA was serially subjected to nested PCR. The first round of PCR was performed with the primers F1 (5'-TTCGCTTCACCTCTGCACG-3') and R1 (5'-AAAGGA CGTCCCGCGCAG-3') for 25 cycles, the products of which were diluted with double distilled water to 1:10, 1:100 and 1:1,000 and used as the template for the second round of PCR with the primers F2 (5'-CGCATGGAGACCACCGTGA-3') and R2 (5'-CACAGCCTAGCAGCCATGG-3'). The nested PCR conditions were as described previously (13) and the products were extracted and sequenced as aforementioned.

According to the sequencing outcome of invPCR conducted above, PCR primers IN F2 (5'-AGGCTGCCTTCC TGTCTG-3') and Alu R2 (5'-CCACGCCCGGCTAATTTT-3') were designed to obtain the left end of the viral-host junction. The primer mix and reaction conditions in PCR were as aforementioned, with extension for 14 sec. The products were extracted and sequenced as aforementioned. As a control, PCR was conducted in both HepG2 and HepG2.2.15 cells.

Reverse transcription-quantitative (RT-q)PCR. RT-qPCR was performed with an OneStep RT-PCR system (Sangon Biotech Co., Ltd.) in HepG2.2.15 cells. The cDNA was synthesized using Sangon cDNA Synthesis kit according to the manufacturer's protocol (Sangon Biotech, Co., Ltd.) using the following reaction conditions: 42˚C for 15 min and 85˚C for 5 min. The expression of HBV-PAK3 fusion transcript was detected using primers IN F1 and IN R1. PCR and sequencing were performed as previously described (11).

Total RNA was extracted from HepG2.2.15 cells with and without H_2O_2 treatment and HepG2 cells and then reverse-transcribed into cDNA as aforementioned. To detect the copy numbers of the chX: 11009033 integration site in HepG2.2.15 cells with and without H_2O_2 treatment, RT-qPCR with the primers IN F1 and IN R1 was performed as described previously (11). PAK3 PCR F (5'-CAACCGGGATTCTT CAGCACT-3') and R primer (5'-CACATGAATCGTATG CTCAAAGTCTG-3') were designed and SYBR Green I (Sangon Biotech Co., Ltd.) was used for RT-qPCR as reported previously (10).

Western blot analysis. Proteins were extracted from HepG2.2.15 cells with and without H_2O_2 treatment and HepG2 cells using Cell Protein Extraction kit according to the manufacturer's instruction (Sangon Biotech Co., Ltd.). GAPDH, (cat. No. AF7021; 1:1,000, Affinity Biosciences) was used as the loading control. Following determination using a Bicinchoninic Acid (BCA) kit according to the manufacturer's instruction (Beyotime Institute of Biotechnology), the cellular proteins (20 μg/lane) were loaded onto 8% SDS-PAGE gels and transferred to PVDF membranes (both Sangon Biotech Co., Ltd.). The membranes were blocked with 5% non-fat milk at 25˚C for 1 h, then incubated with primary antibodies against PAK3 (cat. no. AF7659; 1:1,000, Affinity Biosciences) overnight at 4˚C. Following primary

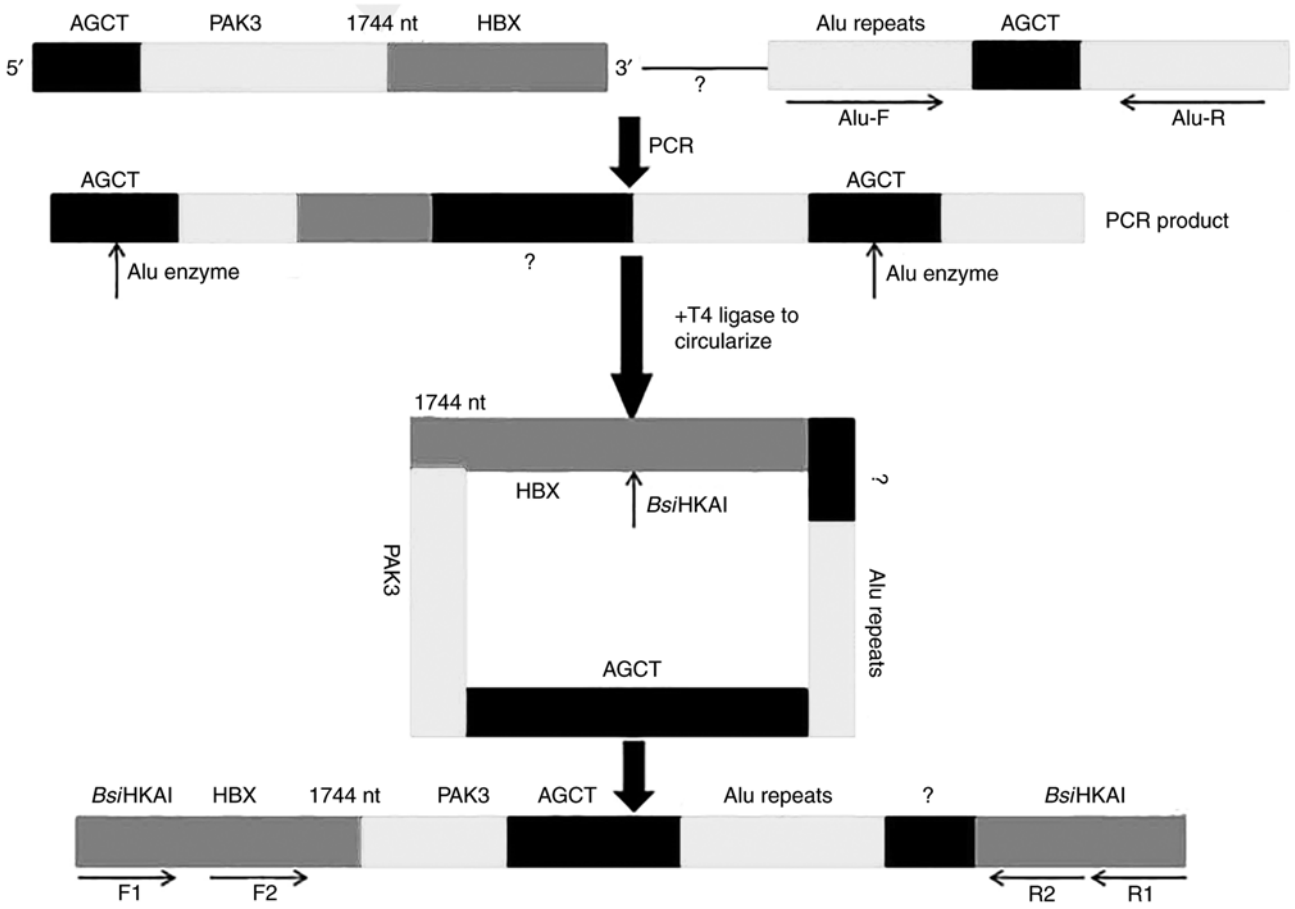

Figure 1. Schematic figure of improved inverse nested PCR assay to detect the full inserted hepatitis B virus genome of the chrX: 11009033 integration site. DNA extracted from HepG2.2.15 cells was amplified by PCR using the primers Cmeric R and Alu F or R. The specific amplificated fragment was digested with Alu, ligated with T4, double digested by *Bsi*HKAI and *SphI*-HF, then amplified by nested PCR. R, reverse; F, forward; nt, nucleotide; PAK3, P21-activated kinase 3.

antibody incubation, the membranes were incubated with secondary antibodies (cat. no. ZB-2305; 1:20,000; OriGene Technologies, Inc.) for 1 h at 25˚C. Finally, protein bands were visualized using ECL Western Blotting Substrate kit according to the manufacturer's protocol (Thermo Fisher Scientific, Inc.), and images were captured for densitometry using ImageJ software (version 1.46; National Institutes of Health).

Statistical analysis. Continuous variables are expressed as the mean ± standard deviation and analyzed by SPSS 20 (IBM Corp.). Student's t test (unpaired) was used to assess differences between two groups; one-way ANOVA followed by Tukey's post hoc test was used for comparison of multiple groups. Correlations were analyzed using Pearson's correlation coefficient. Two-sided $P<0.05$ was considered to indicate a statistically significant difference.

Results

HBV integration site chrX: 111009033 is detected in HepG2.2.15 cells. A fragment of 227 bp was acquired by conventional PCR in DNA extracted from HepG2.2.15 cells (Fig. 2A). BLAST analysis indicated that this was the right end of the junction of the chrX: 111009033 integration site (11).

Full sequence of HBV fragments are detected in the integration site chrX: 111009033. To detect the full HBV integration sequence, improved invPCR was used. Using the primers Chimeric R and Alu R1, a chimeric fragment of 1,255 bp was amplified by conventional PCR (Fig. 2B), which partially contained the Alu repeats. The second round of invPCR specifically amplified a fragment of 900 bp using the product of double digestion diluted 1,000 times (Fig. 2C), as shown by Sanger sequencing (Fig. 3A); the product of the first round of invPCR yielded no product following single digestion (Fig. 2C). To obtain the left end of the HBV-human junction, a pair of PCR primers were designed (IN F2 and Alu R2), by which a fragment of 223 bp was found in HepG2.2.15 but not in HepG2 cells (Fig. 2D). Sanger sequencing indicated that the left HBV-human junction located in 1,228 nt, belonging to HBV P region, and inserted into the Alu repeats with 3 bp (CTG) of shared sequences (Fig. 3B). As a result, it was concluded that the full length of inserted HBV fragment of the chrX: 11009033 integration site was 987 bp, which contained two fragments of dslDNA with the same orientation (1,744-1,094 and 1,565-1,228 nt; Fig. 3C).

Transcription of the chrX: 11009033 integration site and quantitative detection with that of PAK3. HBV-PAK3 chimeric transcript of the chrX: 11009033 integration site

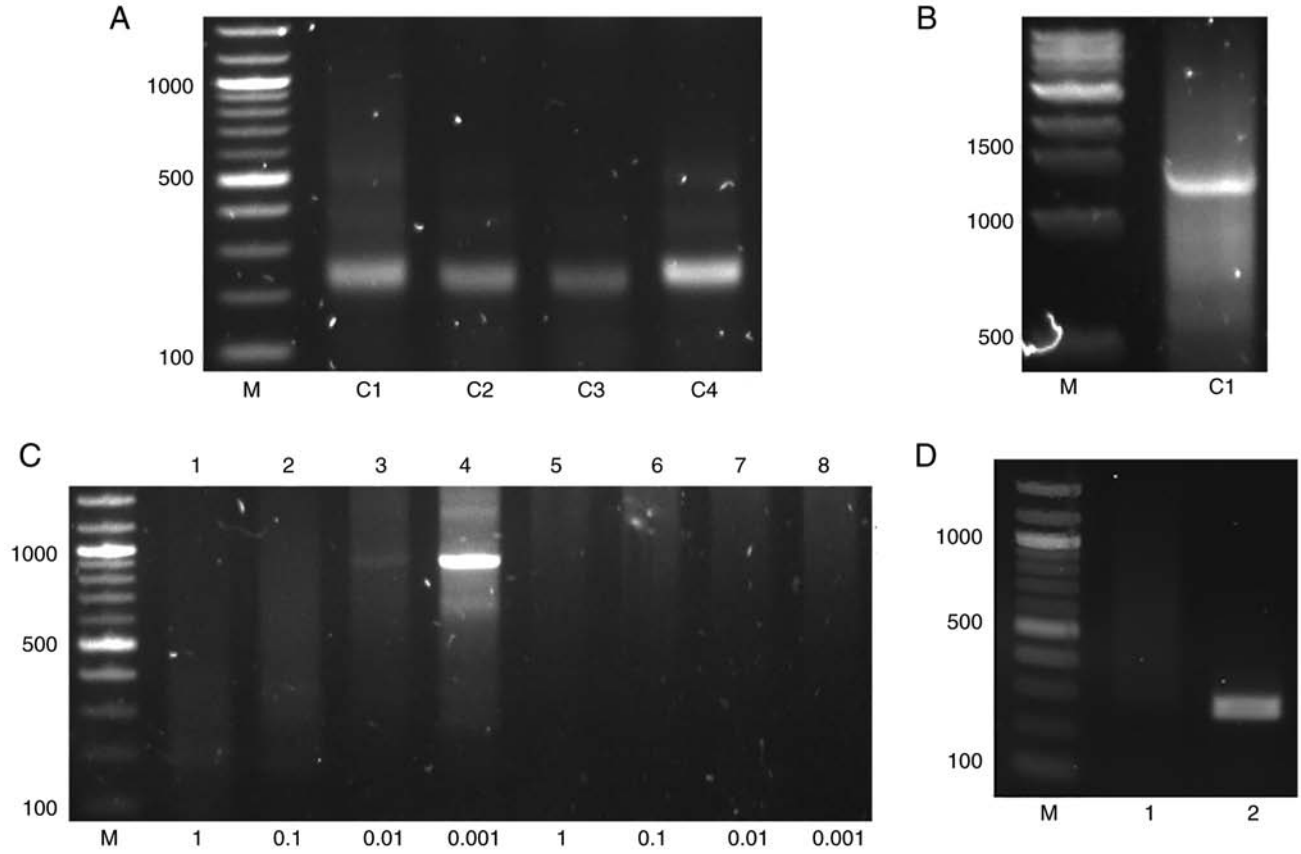

Figure 2. Agarose gel (1.3%) electrophoresis. (A) PCR for the right end of HBV-cell junction in HepG2.2.15 cells. (B) PCR using the primer Chimeric R and Alu R in HepG2.2.15 cells. (C) Inverse nested PCR of DNA extracted from HepG2.2.15 cells double digested by *Bsi*HKAI and *SphI*-HF (1-4) or single digested by *Bsi*HKAI (5-8). (D) PCR for the left end of HBV-cell junction. 1, HepG2; 2, HepG2.2.15 cells. M, DNA marker (DL 100 bp in A, C, D; DL 1,000 bp in B); HBV, hepatitis B virus; R, reverse; DL, DNA Ladder.

was successfully observed in HepG2.2.15 cells by RT-qPCR (Fig. 2A). As H_2O_2 can exacerbate HBV integration (12), copy number of this integration site in cDNA was detected in HepG2.2.15 cells with and without H_2O_2 treatment. Its average level was $3.02x10^{-2}\pm2.33x10^{-2}$ copies/cell (range, $1.36x10^{-3}$-$8.30x10^{-2}$ copies/cell) in cells without H_2O_2 treatment and $8.73x10^{-2}\pm1.65x10^{-2}$ copies/cell ($5.87x10^{-2}$-$1.24x10^{-1}$ copies/cell) in the cells with H_2O_2 treatment with significant difference between them (P<0.0001; Fig. 4A). The level of PAK3 was 15.67±5.65 copies/cell (7.88-26.70 copies/cell) in HepG2.2.15 cells with H_2O_2 treatment, significantly higher than that in the cells without H_2O_2 treatment, 11.34±4.58 copies/cell (4.68-21.30 copies/cell, P=0.0076), and that in HepG2 cells, 5.92±1.54 copies/cell (3.90-9.50 copies/cell, P<0.0001). Significant difference was also found between HepG2.2.15 cells without H_2O_2 treatment and HepG2 cells (P<0.0001, Fig. 4B). The copy numbers of chrX: 11009033 integration site were positively correlated with those of PAK3 (P=0.0013, Fig. 4C).

PAK3 expression is high in HepG2.2.15 cells. To detect protein expression of PAK3, western blotting was performed on HepG2 and HepG2.2.15 cells with and without H_2O_2 treatment (Fig. 5). The overall PAK3 expression was significantly increased in HepG2.2.15 cells with H_2O_2 treatment compared with that in HepG2.2.15 cells without H_2O_2 treatment (37.63±8.16 and 31.38±7.94, P=0.008) and HepG2 cells (21.67±7.88, P<0.0001), while a significant difference was also found between HepG2.2.15 cells without H_2O_2 treatment and HepG2 cells (31.38±7.94 and 21.67±7.88, P=0.0002, Fig. 4D).

Discussion

HepG2.2.15 cells are derived from HepG2 with stable HBV expression (14). Although the HepG2.2.15 cell line may not be used to study the process of HBV infection, it is an ideal tool to study the role of ubiquitination modification on HBV replication, HCC progression and immune tolerance (15). Using HepG2 and HepG2.2.15 cells, molecular mechanisms in hepatocarcinogenesis have been found to cause HBV integration, such as increased apoptosis, DNA hypermethylation and ubiquitylome and proteome modification in host cells (4,15,16). We previously reported the chrX: 11009033 integration site located in the intron of PAK3 gene in HepG2.2.15 cells cultivated in INSERM U1052 (10). Studies have indicated that HBV integration sites are preferentially enriched in the intron of human gene, which may result in host gene dysfunction (17,18). PAKs are serine/threonine protein kinases that are overactivated or overexpressed in many types of tumor including breast cancer, pancreatic melanoma, thyroid cancer (19). PAK3 is a human member of the PAK gene family mapping on chromosome X, which is closely associated with tumor invasion, migration and proliferation (20). The aberrant activation and expression of PAK3 occurs during tumor pathogenesis in gastric

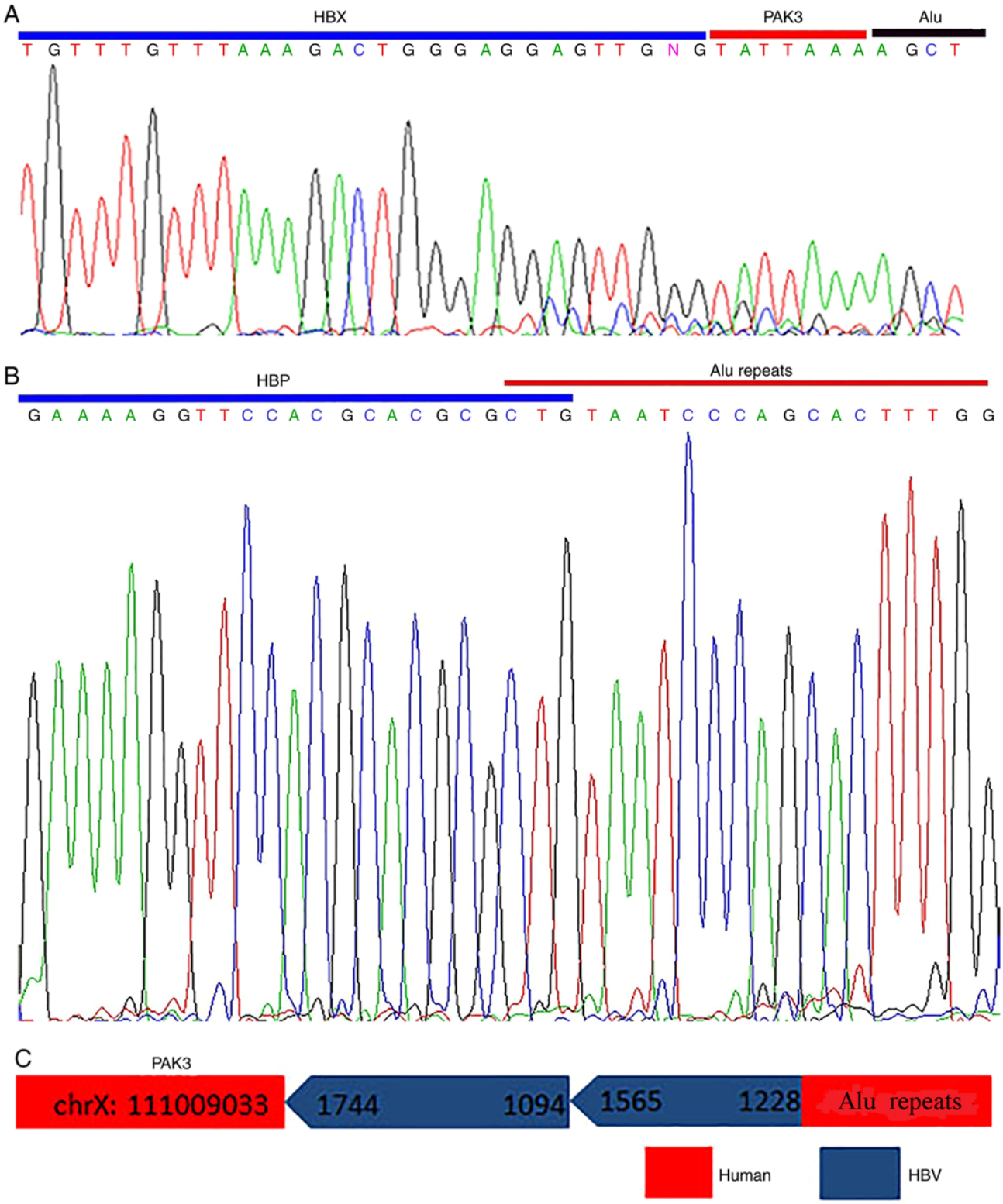

Figure 3. Sanger sequencing and two fragments of HBV DNA in the chrX: 111009033 integration site. (A) Sanger sequencing of the improved inverse nested PCR product. (B) Sanger sequencing of PCR for the left end of HBV-cell junction. (C) Full sequence of HBV DNA fragments of the chrX: 111009033 integration site. HBV, hepatitis B virus; PAK3, P21-activated kinase 3; HBX, HBV X; HBP, HBV P.

and pancreatic cancer, causing it to be considered a tumor enhancer protein (21,22). Epithelial-mesenchymal transition (EMT), a cellular reprogramming process, is key for tumor metastasis and serves a key role in hepatocarcinogenesis by which epithelial cells alter their shape (23). PAK3 serves as an oncogene in HCC by enhancing EMT (10).

In the present study the chrX: 11009033 integration site was detected in HepG2.2.15 cells, indicating this site originated from primary human hepatocyte (PHH) but not from clone hepatocyte and may be an ideal integration event for *in vitro* study (12). Because PAK3 may contribute to HCC, this finding also provides an opportunity to evaluate molecular

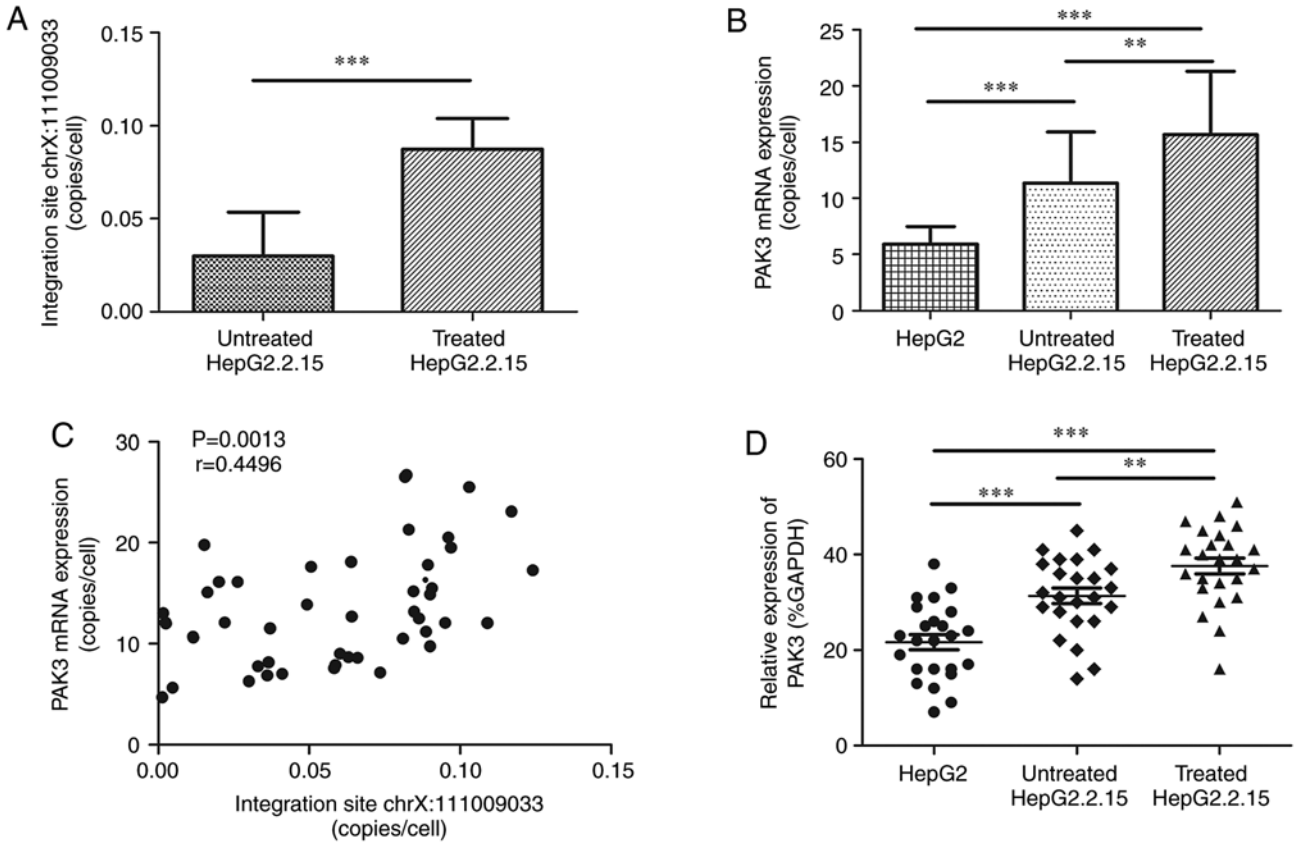

Figure 4. Copies numbers of the integration site chrX: 111009033, PAK3 mRNA and their correlation analysis and protein expression of PAK3. (A) Copy numbers of the integration site chrX: 111009033. (B) Copy numbers of PAK3 mRNA. (C) Correlation analysis between copy numbers of chrX: 111009033 integration sites and PAK3 mRNA. (D) Protein expression of PAK3. PAK3, P21-activated kinase 3. **P<0.01; ***P<0.001.

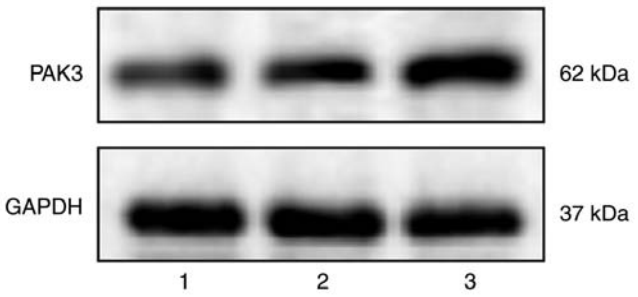

Figure 5. Protein expression of PAK3 in HgpG2.2.15 compared with HepG2 cells, without and with H_2O_2 treatment. PAK3, P21-activated kinase 3.

mechanisms of tumorigenesis of HBV integration. Detection of the full sequence of inserted HBV DNA fragments of this site is difficult by conventional methods. Firstly, the integrated HBV fragments, ranging in size from 28 to 3,215 bp, exist different kinds of rearrangements, such as forward simple junction, reverse simple junction, forward and reverse complicated junctions. Secondly, according to Illumina long-reads sequencing, the presence of structural abnormity of the host genome containing HBV integration results in host genome instability (24-27).

The present study used an improved invPCR technology using *Alu*I instead of *Nco*I restriction enzyme. The invPCR technology can amplify single copies of DNA template with high specificity and sensitivity. An Alu-repeated sequence is interspersed at the average interval of ~4 kb in the human genome, which is often used to amplify unknown flanking sequences (6). To amplify the chimeric fragments, the sequence of which partially aligned to Alu repeats and the unknown integrated HBV genome, two Alu primers with opposite orientation and one chimeric primer were designed, which may be beneficial for Alu digestion and T4 ligation from the two sides of the amplified fragment. Furthermore, double digestion (*Bsi*HKAI and *Sph*I-HF) was performed to avoid non-specific PCR amplification. Dilution step may be key for successful specific amplification in the second round of invPCR. While HBV X region had more integration opportunities than other parts of HBV, the left junction of inserted viral fragments of this site was located in 1,228 nt, providing a novel viral inserting region (HBV P region). On the other hand, 3 bp (CTG) of microhomology homologous (MH) was found, indicating the host chromosomal DNA DSB in this junction was repaired by microhomology-mediated end joining (MMEJ) (28,29). MMEJ is an alternative DNA DSB repair system in mitochondrial DNA lesions (30). As there is enriched MH between HBV and human genome sequences, MMEJ may also be an important mechanism mediating virus integration besides non-homologous end joining (31). Additionally, the presence of HBV-PAK3 chimeric transcripts suggested this integration site may regulate PAK3 gene expression.

E-cadherin is an epithelial marker gene. During HCC progression, hepatocytes lose cell-to-cell contact and acquire migration abilities to spread to distant or surrounding tissue

due to the loss of E-cadherin, thus promoting the invasion and migration of cancer cells (32). The occurrence and promotion of EMT decreases expression of E-cadherin, chiefly via cellular transcription processes involving three transcription factor families: Twist, ZEB and Snail (33). Once activated, these transcription factors can inhibit the expression of epithelial marker genes such as E-cadherin and promote the expression of stromal genes simultaneously (34).

During HCC progression and migration, increased TGF-β signaling is critical for promotion of EMT (35). Smad proteins are downstream targets of TGF-β signaling, which may serve critical roles in proliferation and regulation of transcription and cell differentiation (36). Recent research indicated that in hepatoma cells, PAK3 gene acts through the Smad-dependent TGF-β pathway to enhance EMT (10). In the present study, RT-qPCR and western blot analysis demonstrated that PAK3 was significantly upregulated in HepG2.2.15 cells compared with HepG2 cells, suggesting that the occurrence of HBV integration in HepG2.2.15 cells may affect gene functions such as that of PAK3 (4).

Persistent HBV infection can increase the production of reactive oxygen species in hepatocytes, leading to oxidative damage, host DNA mutation and exacerbating HBV infection (37). This provides opportunity for the selected clonal expansion of HBV-integrated hepatocytes, which may contribute to HCC progression. While H_2O_2 may induce DSB in hepatoma cells (38,39), treating HepG2.2.15 cells with H_2O_2 may mimic ROS production and promote HBV integration (40). Here, the average levels of the chrX: 11009033 integration site and PAK3 expression, which were positively correlated, were significantly higher in HepG2.2.15 cells with H_2O_2 treatment compared with the cells without treatment. Multiple factors may contribute to upregulation of PAK3 expression in HepG2.2.15 cells, including occurrence and clonal expansion of chrX: 11009033 integration site, as shown by the significant difference in levels of PAK3 between HepG2 and HepG2.2.15 cells and its positive correlation with chrX: 11009033 integration site in the latter. The mechanism at the molecular level underlying the functions of EMT and TGF-β/Smad signaling need to be further investigated.

In summary, the chrX: 11009033 integration site, originated from PHH and may be an ideal integration event for *in vitro* study. The full length of inserted HBV fragment of this site was 987 bp, containing two fragments of dslDNA with the same orientation. The occurrence of the chrX: 11009033 integration site and its clonal expansion may upregulate PAK3 expression and serve a role in hepatocarcinogenesis. Further investigation is required to determine its molecular mechanisms.

Acknowledgements

Not applicable.

Funding

The present study was supported by the National Natural Science Foundation of Hubei Province (grant no. 2020CFB608).

Availability of data and materials

The datasets used and/or analyzed during the present study are available from the corresponding author on reasonable request.

Authors' contributions

PR and JS confirm the authenticity of all the raw data, designed and conceived the study. PR, RZ and HSY conducted cell culture and molecular biological experiments. MJL and CH performed western blot experiments. CPH and XFD conducted the statistical analysis. PR wrote the manuscript. All authors have read and approved the final manuscript.

Ethics approval and consent to participate

Not applicable.

Patient consent for publication

Not applicable.

Competing interests

The authors declare that they have no competing interests.

References

1. GBD 2016 Causes of Death Collaborators: Global, regional, and national age-sex specific mortality for 264 causes of death, 1980-2016: A systematic analysis for the global burden of disease study 2016. Lancet 390: 1151-1210, 2017.
2. Ruan P, Zhou B, Dai X, Sun Z, Guo X, Huang J and Gong Z: Predictive value of intrahepatic hepatitis B virus covalently closed circular DNA and total DNA in patients with acute hepatitis B and patients with chronic hepatitis B receiving anti-viral treatment. Mol Med Rep 9: 1135-1141, 2014.
3. Lin SY, Zhang A, Lian J, Wang J, Chang TT, Lin YJ, Song W and Su YH: Recurrent HBV integration targets as potential drivers in hepatocellular carcinoma. Cells 10: 1294, 2021.
4. Hu X, Jiang J, Ni C, Xu Q, Ye S, Wu J, Ge F, Han Y, Mo Y, Huang D and Yang L: HBV integration-mediated cell apoptosis in HepG2.2.15. J Cancer 10: 4142-4150, 2019.
5. Tu T, Budzinska MA, Vondran FWR, Shackel NA and Urban S: Hepatitis B virus DNA integration occurs early in the viral life cycle in an in vitro infection model via sodium taurocholate cotransporting polypeptide-dependent uptake of enveloped virus particles. J Virol 92: e020007-17, 2018.
6. Minami M, Poussin K, Bréchot C and Paterlini P: A novel PCR technique using Alu-specific primers to identify unknown flanking sequences from the human genome. Genomics 29: 403-408, 1995.
7. Ding D, Lou X, Hua D, Yu W, Li L, Wang J, Gao F, Zhao N, Ren G, Li L and Lin B: Recurrent targeted genes of hepatitis B virus in the liver cancer genomes identified by a next-generation sequencing-based approach. PLoS Genet 8: e1003065, 2012.
8. Lau CC, Sun T, Ching AK, He M, Li JW, Wong AM, Co NN, Chan AW, Li PS, Lung RW, *et al*: Viral-human chimeric transcript predisposes risk to liver cancer development and progression. Cancer Cell 25: 335-349, 2014.
9. Svicher V, Salpini R, Piermatteo L, Carioti L, Battisti A, Colagrossi L, Scutari R, Surdo M, Cacciafesta V, Nuccitelli A, *et al*: Whole exome HBV DNA integration is independent of the intrahepatic HBV reservoir in HBeAg-negative chronic hepatitis B. Gut 70: 2337-2348, 2021.
10. Gao Z, Zhong M, Ye Z, Wu Z, Xiong Y, Ma J, Chen H, Zhu Y, Yang Y, Zhao Y and Zhang Z: PAK3 promotes the metastasis of hepatocellular carcinoma by regulating EMT process. J Cancer 13: 153-161, 2022.
11. Ruan P, Dai X, Sun J, He C, Huang C, Zhou R and Chemin I: Integration of hepatitis B virus DNA into p21-activated kinase 3 (PAK3) gene in HepG2.2.15 cells. Virus Genes 56: 168-173, 2022.
12. Dandri M, Burda MR, Bürkle A, Zuckerman DM, Will H, Rogler CE, Greten H and Petersen J: Increase in de novo HBV DNA integrations in response to oxidative DNA damage or inhibition of poly(ADP-ribosyl)ation. Hepatology 35: 217-223, 2002.

13. Tu T and Jilbert AR: Detection of hepatocyte clones containing integrated hepatitis B virus DNA using inverse nested PCR. Methods Mol Biol 1540: 97-118, 2017.
14. Sells MA, Chen ML and Acs G: Production of hepatitis B virus particles in Hep G2 cells transfected with cloned hepatitis B virus DNA. Proc Natl Acad Sci USA 84: 1005-1009, 1987.
15. Yuan S, Tanzeel Y, Tian X, Zheng D, Wajeeha N, Xu J, Ke Y, Zhang Z, Peng X, Lu L, *et al*: Global analysis of HBV-mediated host proteome and ubiquitylome change in HepG2.2.15 human hepatoblastoma cell line. Cell Biosci 11: 75, 2021.
16. Oikawa R, Watanabe Y, Yotsuyanagi H, Yamamoto H and Itoh F: DNA methylation at hepatitis B virus integrants and flanking host mitochondrially encoded cytochrome C oxidase III. Oncol Lett 24: 424, 2022.
17. Yan H, Yang Y, Zhang L, Tang G, Wang Y, Xue G, Zhou W and Sun S: Characterization of the genotype and integration patterns of hepatitis B virus in early- and late-onset hepatocellular carcinoma. Hepatology 61: 1821-1831, 2015.
18. Li W, Cui X, Huo Q, Qi Y, Sun Y, Tan M and Kong Q: Profile of HBV integration in the plasma DNA of hepatocellular carcinoma patients. Curr Genomics 20: 61-68, 2019.
19. Ye DZ and Field J: PAK signaling in cancer. Cell Logist 2: 105-116, 2012.
20. Zhou N, Ding B, Agler M, Cockett M and McPhee F: Lethality of PAK3 and SGK2 shRNAs to human papillomavirus positive cervical cancer cells is independent of PAK3 and SGK2 knockdown. PLoS One 10: e0117357, 2015.
21. Wang GJ, Yu TY, Li YR, Liu YJ and Deng BB: Circ_0000190 suppresses gastric cancer progression potentially via inhibiting miR-1252/PAK3 pathway. Cancer Cell Int 20: 351, 2020.
22. Wu HY, Yang MC, Ding LY, Chen CS and Chu PC: p21-activated kinase 3 promotes cancer stem cell phenotypes through activating the Akt-GSK3β-β-catenin signaling pathway in pancreatic cancer cells. Cancer Lett 456: 13-22, 2019.
23. Santamaria PG, Moreno-Bueno G, Portillo F and Cano A: EMT: Present and future in clinical oncology. Mol Oncol 11: 718-738, 2017.
24. Hama N, Totoki Y, Miura F, Tatsuno K, Saito-Adachi M, Nakamura H, Arai Y, Hosoda F, Urushidate T, Ohashi S, *et al*: Epigenetic landscape influences the liver cancer genome architecture. Nat Commun 9: 1643, 2018.
25. Mason WS, Low HC, Xu C, Aldrich CE, Scougall CA, Grosse A, Clouston A, Chavez D, Litwin S, Peri S, *et al*: Detection of clonally expanded hepatocytes in chimpanzees with chronic hepatitis B virus infection. J Virol 83: 8396-8408, 2009.
26. Yang L, Ye S, Zhao X, Ji L, Zhang Y, Zhou P, Sun J, Guan Y, Han Y, Ni C, *et al*: Molecular characterization of HBV DNA integration in patients with hepatitis and hepatocellular carcinoma. J Cancer 9: 3225-3235, 2018.
27. Ruan P, Dai XF, Sun J, He C, Huang C, Zhou R, Cao Z and Ye L: Different types of viral-host junction found in HBV integration breakpoints in HBV-infected patients. Mol Med Rep 19: 1410-1416, 2019.
28. Li W, Zeng X, Lee NP, Liu X, Chen S, Guo B, Yi S, Zhuang X, Chen F, Wang G, *et al*: HIVID: An efficient method to detect HBV integration using low coverage sequencing. Genomics 102: 338-344, 2013.
29. Hu Z, Zhu D, Wang W, Li W, Jia W, Zeng X, Ding W, Yu L, Wang X, Wang L, *et al*: Genome-wide profiling of HPV integration in cervical cancer identifies clustered genomic hot spots and a potential microhomology-mediated integration mechanism. Nat Genet 47: 158-163, 2015.
30. Tadi SK, Sebastian R, Dahal S, Babu RK, Choudhary B and Raghavan SC: Microhomology-mediated end joining is the principal mediator of double-strand break repair during mitochondrial DNA lesions. Mol Biol Cell 27: 223-235, 2016.
31. Lamouille S, Xu J and Derynck R: Molecular mechanisms of epithelial-mesenchymal transition. Nat Rev Mol Cell Biol 15: 178-196, 2014.
32. Mladenov E, Magin S, Soni A and Iliakis G: DNA double-strand-break repair in higher eukaryotes and its role in genomic instability and cancer: Cell cycle and proliferation-dependent regulation. Semin Cancer Biol 37-38: 51-64, 2016.
33. Thiery JP: Epithelial-mesenchymal transitions in development and pathologies. Curr Opin Cell Biol 15: 740-746, 2003.
34. Gui Y, Khan MGM, Bobbala D, Dubois C, Ramanathan S, Saucier C and Ilangumaran S: Attenuation of MET-mediated migration and invasion in hepatocellular carcinoma cells by SOCS1. World J Gastroenterol 23: 6639-6649, 2017.
35. Zhang C, Zhang X, Xu R, Huang B, Chen AJ, Li C, Wang J and Li XG: TGF-β2 initiates autophagy via Smad and non-Smad pathway to promote glioma cells' invasion. J Exp Clin Cancer Res 36: 162, 2017.
36. Ahmadi A, Najafi M, Farhood B and Mortezaee K: Transforming growth factor-β signaling: Tumorigenesis and targeting for cancer therapy. J Cell Physiol 234: 12173-12187, 2019.
37. Zhao LH, Liu X, Yan HX, Li WY, Zeng X, Yang Y, Zhao J, Liu SP, Zhuang XH, Lin C, *et al*: Genomic and oncogenic preference of HBV integration in hepatocellular carcinoma. Nat Commun 7: 12992, 2016.
38. Schraufstatter IU, Hyslop PA, Hinshaw DB, Spragg RG, Sklar LA and Cochrane CG: Hydrogen peroxide-induced injury of cells and its prevention by inhibitors of poly(ADP-ribose) polymerase. Proc Natl Acad Sci USA 83: 4908-4912, 1986.
39. Schraufstatter IU, Hyslop PA, Jackson J and Cochrane CC: Oxidant injury of cells. Int J Tissue React 9: 317-324, 1987.
40. Mason WS, Jilbert AR and Summers J: Clonal expansion of hepatocytes during chronic woodchuck hepatitis virus infection. Proc Natl Acad Sci USA 102: 1139-1144, 2005.